



Star formation from gravoturbulent fragmentation: mass accretion and evolution of protostars

S. Schmeja¹, R. S. Klessen¹, D. Froebrich² and M. D. Smith³

¹ Astrophysikalisches Institut Potsdam, An der Sternwarte 16, D-14482 Potsdam, Germany
e-mail: sschmeja@aip.de

² Dublin Institute for Advanced Studies, 5 Merrion Square, Dublin 2, Ireland

³ Armagh Observatory, College Hill, Armagh BT61 9DG, Northern Ireland

Abstract. We present numerical simulations of the fragmentation and collapse of turbulent, self-gravitating molecular clouds. Protostellar mass accretion rates are highly time-variable and are correlated with the final stellar mass as well as with the turbulent flow velocity of the environment. Combining the accretion rates with an evolutionary scheme allows us to determine T_{bol} , L_{bol} , and M_{env} and generate evolutionary tracks for the model protostars. The distribution of our model stars in the $T_{\text{bol}}\text{-}L_{\text{bol}}\text{-}M_{\text{env}}$ parameter space is compared with that of a sample of all known Class 0 sources. Finally, we investigate the number ratios of young stars belonging to different evolutionary classes in the numerical models and compare them to those in observed star-forming clusters.

Key words. hydrodynamics – stars: formation – accretion, accretion disks

1. Introduction

Stars form by the fragmentation and gravitational collapse of dense cores of interstellar molecular clouds. The star formation process is controlled by the complex interplay between gravity and supersonic turbulence (see Mac Low & Klessen 2004 for a review). Supersonic turbulence, which is observed ubiquitously throughout the Galaxy, plays a dual role: On large scales it counterbalances gravity and prevents the molecular cloud from collapsing, while on small scales it can produce strong density enhancements that eventually lead to local collapse and the for-

mation of protostars. The turbulence is driven on scales substantially larger than the clouds themselves. In the case of the Milky Way it is probably caused by supernova explosions, in other types of galaxies it might be also due to magnetorotational or gravitational instabilities. Once a gas clump becomes gravitationally unstable, it begins to collapse and the central density increases considerably until a protostellar core forms in the centre, which grows in mass by accretion from the infalling envelope.

2. Numerical simulations

We perform numerical simulations of the fragmentation and collapse of turbulent, self-

Send offprint requests to: S. Schmeja

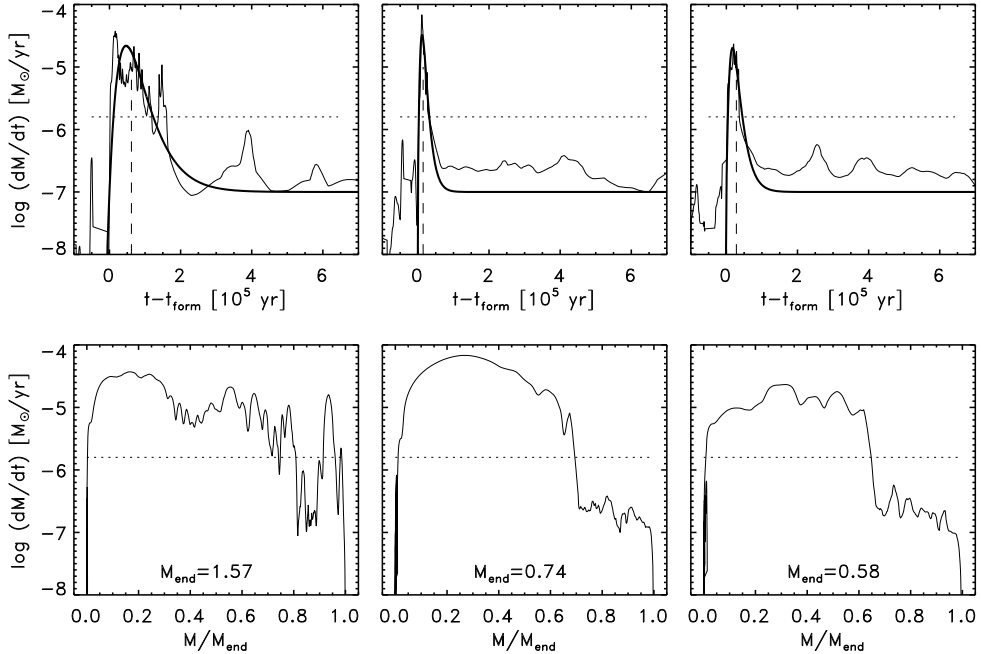


Fig. 1. Mass accretion history of three individual protostellar cores of model M6k2a versus time after formation (upper panel). The thin line represents the actual simulation, the thick line the fit as described in the text. The dotted line shows the constant accretion rate predicted by the “standard model” (Shu 1977). The dashed line stands for the assumed transition from Class 0 to Class 1 (when $M_* = 0.43M_{\text{end}}$, Schmeja et al. 2004). The lower panel shows the same objects as above plotted versus the ratio of accreted to final mass. The final masses are displayed in M_{\odot} .

gravitating molecular clouds and the resulting formation and evolution of protostars (Schmeja & Klessen 2004). We use an SPH (smoothed particle hydrodynamics) code with an isothermal equation of state, periodic boundary conditions and sink particles that replace high-density cores while keeping track of mass and linear and angular momentum. Our simulations consist of two globally unstable models that contract from Gaussian initial conditions without turbulence and of 22 models where turbulence is maintained with constant rms Mach numbers \mathcal{M} , in the range $0.1 \leq \mathcal{M} \leq 10$. We distinguish between turbulence that carries its energy mostly on large scales, at wavenumbers $1 \leq k \leq 2$, on intermediate scales, i.e. $3 \leq k \leq 4$, and on small scales with $7 \leq k \leq 8$. The models are computed in normalised units. Scaled to physical units we adopt a tem-

perature of 11.3 K corresponding to a sound speed $c_s = 0.2 \text{ km s}^{-1}$, and a mean density of $n(\text{H}_2) = 10^5 \text{ cm}^{-3}$. The total mass in the two Gaussian models is $220 M_{\odot}$, and the size of the cube is 0.34 pc . The turbulent models have a mass of $120 M_{\odot}$ within a volume of $(0.28 \text{ pc})^3$. The mean thermal Jeans mass in all models is $\langle M_J \rangle = 1 M_{\odot}$, and the global free-fall timescale is $\tau_{\text{ff}} = 10^5 \text{ yr}$. Requiring that the local Jeans mass is always resolved by at least 100 gas particles (Bate & Burkert 1997) the resolution limit in all considered turbulent models is $0.058 M_{\odot}$, and $0.044 M_{\odot}$ in the Gaussian model. Details on the individual models are given in Table 1 of Schmeja & Klessen (2004). In the figures here the model M6k2a with $\mathcal{M} = 6$ and $1 \leq k \leq 2$ is shown.

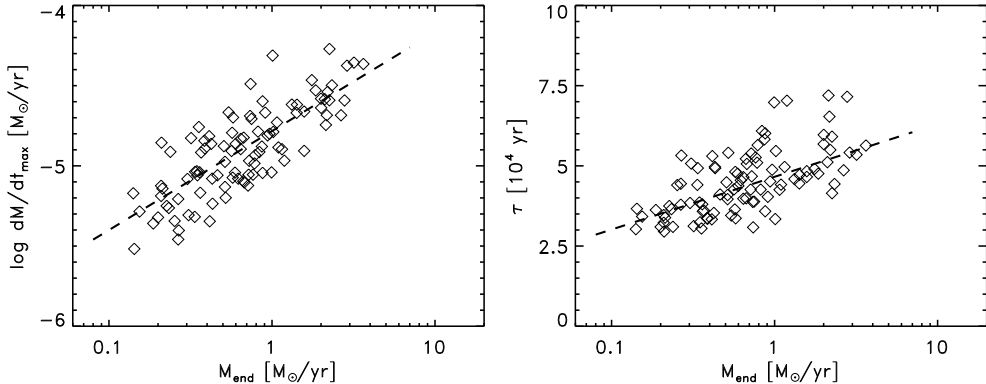


Fig. 2. Peak accretion rates $\log \dot{M}_{\max}$ (left) and time τ (right) for all protostars of model M6k2a versus final stellar mass. The dashed line shows a linear fit.

3. Mass accretion rates

A simple approximation to the mass accretion rate \dot{M} can be obtained by dividing the local Jeans mass by the local dynamical timescale:

$$\dot{M} \approx M_J/\tau_{\text{ff}} = 5.4 \frac{c_s^3}{G}, \quad (1)$$

with the isothermal sound speed c_s and the gravitational constant G . This gives a higher value than the constant accretion rate for the collapse of a singular isothermal sphere (Shu 1977). However, protostellar mass accretion rates from the models are highly time-variant (Fig. 1). They show a sharp peak during the Class 0 stage, shortly after the protostellar core has formed. Later they show an approximately exponential decline. Due to the dynamical interaction and competition between protostellar cores, there are secondary accretion peaks.

Around the peak accretion phase \dot{M} is roughly constant. We define mean accretion rates $\langle \dot{M} \rangle$ in the range $0.1 \leq M/M_{\text{end}} \leq 0.8$. This phase typically lasts only a few 10^4 years, which is very short compared to the duration of the entire accretion phase. The majority of the material is accrued onto the star in the short time span while the system is close to maximum accretion. For each of the models the mean accretion rates $\langle \dot{M} \rangle$ of all protostars are averaged. Those averaged mean accretion rates $\langle \dot{M} \rangle_{\text{mean}}$ show a negative correlation with

the Mach number of the turbulent environment (Schmeja & Klessen 2004). The stronger support of the turbulent medium against collapse typically results in a lower mean accretion rate.

The accretion history can be described by the empirical fit formula

$$\log \dot{M}(t) = \log \dot{M}_0 \frac{e}{\tau} t e^{-t/\tau} \quad (2)$$

with time t and the fit parameters $\log \dot{M}_0$ and τ . This holds for the following conditions: We shift the ordinate by $\Delta \log \dot{M}/(M_{\odot} \text{ yr}^{-1}) = +7$ and we consider accretion when $\log \dot{M} \geq -7$. The fitted curves are plotted as thick lines in Fig. 1. Note that the axes display the original values without the applied shifts. If there are secondary accretion peaks, they are typically ignored and levelled out by the routine.

The fit parameter $\log \dot{M}_0 - 7$, hereafter denoted as $\log \dot{M}_{\max}$, gives the value of the peak accretion. It is in the range $5 \times 10^{-6} \lesssim \dot{M}_{\max} \lesssim 10^{-4} M_{\odot} \text{ yr}^{-1}$ and it is correlated with the final mass M_{end} of the star (Fig. 2). The parameter τ indicates the time when the peak accretion is reached, it is shown in the right panel of Fig. 2. This parameter is related with the local free-fall time and thus the local density at the onset of collapse. On average, τ is about one third of the global free-fall time, suggesting an initial overdensity of about a factor of ten in the collapsing regions.

From observations it is estimated that \dot{M} falls from $\sim (0.1-1) \times 10^{-4} M_{\odot} \text{ yr}^{-1}$ for Class 0

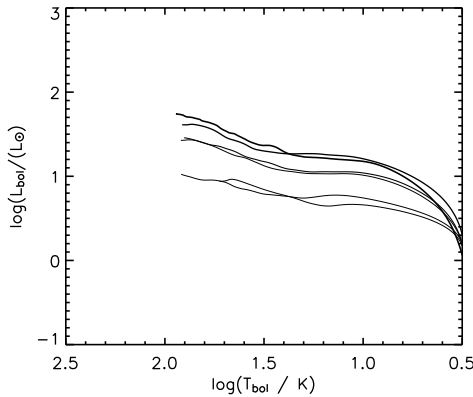


Fig. 3. Evolutionary tracks for all protostars of model M6k2a until the end of Class 0 phase, averaged in six mass bins. Thicker lines correspond to higher final masses.

protostars to $\lesssim 10^{-6} M_{\odot} \text{ yr}^{-1}$ for Class 1 objects (e.g. Bontemps et al. 1996; see also the discussion in Schmeja & Klessen 2004). This corresponds to the values derived from our models, however, the values from the observations are usually not measured directly, but have to be inferred by indirect methods. Thus, it is desirable to convert the obtained mass accretion rates to easier observable quantities, such as bolometric luminosity L_{bol} or bolometric temperature T_{bol} .

4. Evolutionary tracks

We combine the mass accretion rates from the gravoturbulent models with an evolutionary code (Smith 2000), which allows us to determine T_{bol} , L_{bol} , and the envelope mass M_{env} and generate evolutionary tracks for the model protostars. All tracks show a similar behaviour: A steep increase in L_{bol} until $T \approx 10 \text{ K}$ is followed by a slower increase in luminosity until the end of Class 0 phase. Most protostars reach the transition to Class 1 at $T_{\text{bol}} \approx 80 \text{ K}$. Evolutionary tracks for Class 0 protostars of one model, determined from the mean accretion rate in six mass bins, are shown in Fig. 3. The general behaviour is the same for all models: There is a correlation between the position of the tracks and the final mass (higher

final masses lead to a higher bolometric luminosity). However, when considering the scatter of the individual tracks, it turns out that the final mass of an object cannot be determined from the measured L_{bol} and T_{bol} more accurately than by a factor of four. The position of a protostar in the $T_{\text{bol}}-L_{\text{bol}}$ diagram is primarily determined by the accretion history and not by its final mass. Unlike in the pre-main sequence phase, there are no unique evolutionary tracks in the Class 0 phase.

The distribution of our model stars in the $T_{\text{bol}}-L_{\text{bol}}-M_{\text{env}}$ parameter space is compared with that of a sample of all known Class 0 sources (Froebrich 2005) by means of a 3D Kolmogorov-Smirnov test to constrain the parameters of the gravoturbulent models and the evolutionary code. The probability that the modelled and the observed distribution are drawn from the same basic population varies strongly for the different models, in the best case it is 36%. This value is rather low, but of course it is influenced by a limited and probably biased observational sample on one hand, and too simple assumptions in the gravoturbulent models and the evolutionary code on the other hand. No correlation of the result with the turbulent environment or the initial mass function is found (Froebrich et al. 2004).

All Class 0 objects in Taurus are underluminous compared to the other sources (Froebrich 2005), consequently showing a poorer agreement with the model tracks. These objects appear to undergo a different accretion history, which might indicate that star formation in Taurus is locally more strongly influenced by magnetic fields than in other star-forming regions. For a detailed discussion see Froebrich et al. (2004).

5. YSO ratios in clusters

Embedded clusters usually contain young stellar objects (YSOs) belonging to different evolutionary classes, from embedded Class 0 sources to relatively evolved Class 3 pre-main sequence stars. We compile the numbers of YSOs in these classes in seven star-forming clusters from the literature (Schmeja et al. 2004). The relative numbers are compared to

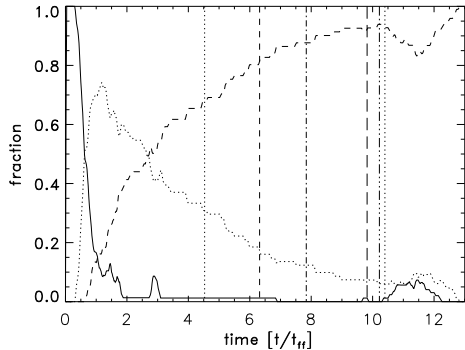


Fig. 4. Temporal evolution of the relative YSO numbers in model M6k2a. (Solid line: Class 0, dotted line: Class 1, dashed line: Class 2+3). The vertical lines indicate the time, when the model shows the best agreement with the observations of Serpens (dotted), NGC 7129 (dashed), Taurus and IC 1396A (dash-dotted), ρ Ophiuchi (long dashes), Cha I (dash dot dot dot), and IC 348 (second dotted line).

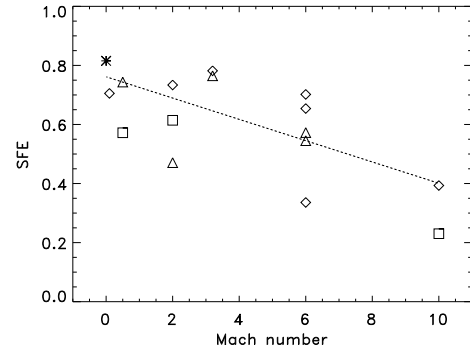


Fig. 5. Star formation efficiency at the best-fit time for ρ Oph versus the Mach numbers of all models. The symbols indicate the wave numbers $1 \leq k \leq 2$ (diamonds), $3 \leq k \leq 4$ (triangles), and $7 \leq k \leq 8$ (squares). The Gaussian collapse model is displayed as an asterisk. The dotted line shows a linear fit to the data (false alarm probability $< 0.5\%$).

our gravoturbulent models, which describe the entire collapse of a molecular cloud core and build-up of a stellar cluster as a function of time. This permits to constrain the models and possibly to determine the evolutionary stage of the cluster by comparison with the models.

Fig. 4 shows the temporal evolution of the fractions of YSO classes in the model M6k2a. The time t_{fit} of the best agreement between observations and models is determined by the minimum weighted root mean square of the differences. The best-fit times are shown as vertical lines in Fig. 4. They vary with the different models, but all models show the same evolutionary sequence: $t(\text{Ser}) < t(\text{NGC 7129}) < t(\text{IC 1396A}) \leq t(\text{Tau}) < t(\rho \text{ Oph}) < t(\text{Cha I}) < t(\text{IC 348})$.

We determine the star formation efficiency (SFE) of the models at time t_{fit} . Fig. 5 shows the SFE for the best-fit time of ρ Oph plotted versus the Mach numbers of all models. There is an inverse correlation of the SFE with the Mach number. This is probably due to the fact that in high-Mach number turbulence less mass is available for collapse at the sonic scale (Vázquez-Semadeni et al. 2003). If we inter-

pret the measured velocity dispersions in the clusters as the result of turbulence, we can estimate the SFEs at time t_{fit} for the particular Mach numbers from Fig. 5. The SFE then is ~ 0.27 in ρ Oph ($M > 10$), and between 0.60 and 0.65 in Serpens, Taurus, Cha I, and NGC 7129 ($1 \lesssim M \lesssim 4$). These values are significantly higher than the measured SFEs, which are only around 0.1. Only in the case of ρ Oph the SFE of the models is in the range of the SFE measured in dense subclusters. The main reasons for this discrepancy are probably the limitation of the gas reservoir and the neglect of outflows and feedback mechanisms in the simulations.

6. Conclusions

Protostellar mass accretion is a stochastic and highly time-varying process. Accretion rates from gravoturbulent models show a sharp peak shortly after the formation of the protostar, followed by a slower decline. The mass accretion history can be approximated by an empirical exponential equation. The mean accretion rates are correlated with the final stellar mass and in-

versely correlated with the rms Mach number of the turbulent medium.

Combining the accretion rates with an evolutionary scheme shows that individual evolutionary tracks are largely determined by the accretion history and not by the final mass. Unlike the pre-main sequence phase, no unique evolutionary tracks exist for Class 0 protostars. Hence, mass estimates are possible only by a factor of four. A 3D Kolmogorov-Smirnov test was applied to compare the model tracks with an observational sample of Class 0 objects. The highest probability that both distributions are drawn from the same basic population is 36%, there is no correlation with the parameters of the turbulent environment.

Comparing the observed numbers of YSOs belonging to different evolutionary classes allows us to derive a sequence for the ages of star-forming regions, revealing Serpens as the youngest, and IC 348 as the most evolved of the seven investigated clusters. We find an inverse correlation between the star formation efficiency and the Mach number of the turbulence. However, the observed SFE can only be reproduced for highly turbulent ($\mathcal{M} > 10$) regions by the present models.

Acknowledgements. The work of SS and RSK is funded by the *Emmy Noether Programme* of the *Deutsche Forschungsgemeinschaft* (grant no.

KL1358/1). DF is supported by the *Cosmo-Grid* project, funded by the Program for Research in Third Level Institutions under the National Development Plan and with assistance from the European Regional Development Fund. MDS thanks the Department of Culture, Arts and Leisure (Northern Ireland). This publication makes use of the Protostars Webpage (www.dias.ie/protostars/) hosted by the Dublin Institute for Advanced Studies.

References

- Bate, M.R. & Burkert, A. 1997, MNRAS 288, 1060
- Bontemps, S., André, P., Terebey, S. & Cabrit, S. 1996, A&A 311, 858
- Froebrich, D. 2005, ApJS in press
- Froebrich, D., Schmeja, S., Smith, M.D. & Klessen, R.S. 2004, A&A submitted
- Mac Low, M.-M. & Klessen, R.S. 2004, Rev. Mod. Phys. 76, 125
- Schmeja, S. & Klessen, R.S. 2004, A&A 419, 405
- Schmeja, S., Klessen, R.S. & Froebrich, D. 2004, A&A submitted
- Shu, F.H. 1977, ApJ 214, 488
- Smith, M.D. 2000, Ir. Astron. J. 27, 25
- Vázquez-Semadeni, E., Ballesteros-Paredes, J. & Klessen, R.S. 2003, ApJ 585, L131